FULL PAPER

Bulky PNP ligands blocking metal-ligand cooperation allow for isolation of Ru(0), and lead to catalytically active Ru complexes in acceptorless alcohol dehydrogenation

Shubham Deolka,[a] Robert R. Fayzullin,[b] Eugene Khaskin*[a]

[a] S. Deolka, E. Khaskin.
Okinawa Institute of Science and Technology Graduate University
Onna-son, Kunigami-gun, Okinawa, Japan, 904-0495
E-mail: eugene.khaskin@oist.jp
[b] R. R. Fayzullin
Abuzov Institute of Organic and Physical Chemistry, FRC Kazan Scientific Center of RAS
8 Arbuzov Street, Kazan 420088, Russian Federation

Supporting information for this article is given via a link at the end of the document.

Abstract: We synthesized two 4Me-PNP ligands which block metal-ligand cooperation (MLC) with the Ru center and compared their Ru complex chemistry to their two traditional analogues used in acceptorless alcohol dehydrogenation catalysis. The corresponding 4Me-PNP complexes, which do not undergo dearomatization upon addition of base, allowed us to obtain rare, albeit unstable, 16 electron mono CO Ru(0) complexes. Reactivity with CO and H_2 allows for stabilization and extensive characterization of bis CO Ru(0) 18 electron and Ru(II) cis and trans dihydride species that were also shown to be capable of C(sp2)-H activation. Reactivity and catalysis are contrasted to non-methylated Ru(II) species, showing that an MLC pathway is not necessary, with dramatic differences in outcomes during catalysis between ^{i}Pr and ^{t}Bu PNP complexes within each of the 4Me and non-methylated backbone PNP series being observed. Unusual intermediates are characterized in one of the new and one of the traditional complexes, and a common catalysis deactivation pathway was identified.

Introduction

Ruthenium complex catalyzed acceptorless dehydrogenative coupling of alcohols to esters and the reverse hydrogenation of esters performed under H_2 pressure is now a commonly established reaction since its description under mild conditions by Milstein in 2005/6 (Eq. 1). [1]

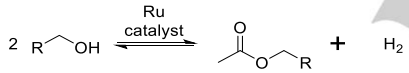

Equation 1 General Catalytic reaction.

Since those reports, Ru pincer complexes have been reported to be active in a number of related reactions such as: the synthesis of amides from alcohols and amines[2] and the reverse reaction;[3] synthesis of imines from alcohols and amines;[4] secondary amines from alcohols and primary amines/ammonia;[5] acceptorless transformation of alcohols to carboxylic acids with water;[6] CO_2 reduction;[7] thioester alcohols;[8] cross coupling of alcohols;[9] and the introduction of alcohols as a substrate in reactions normally requiring aldehydes,[10] sometimes enabling novel reactivity. [11] Ideally, all these reactions can be used in the synthesis of bulk chemicals, or for pharmaceutical intermediates and fine chemicals in the chemical industry. The promiscuity of the catalysts often comes with the major drawback of non-selectivity and undesired side reactions with functional groups. The design of catalytic systems that work at temperatures and pressures close to ambient conditions and improve selectivity is a major goal of current research efforts. In ester hydrogenation, this has already led to recent reports of complexes that are highly active at temperatures of <100°C and can achieve at least several thousand turnovers.[12] Concurrently, the mechanism of these transformations continues to be examined in detail.

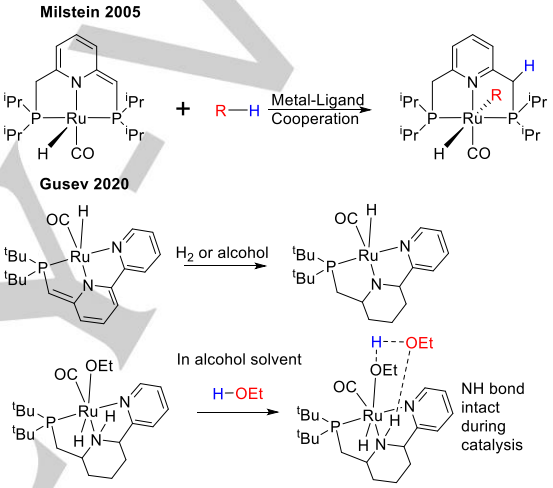

Scheme 1 Proposed MLC mechanism contrasted to ligand assisted substrate activation.

Some of the first crucial steps of the original Milstein system's catalytic cycle are believed to be dearomatization of the central pyridine ring after deprotonation by base, and re-aromatization by substrate addition across the ligand arm and metal center (i.e. Metal-Ligand Cooperation or MLC) (Scheme 1). [1d],[13]

A number of recent studies have found that pyridine supported Ru complexes can hydrogenate the pyridine ring during catalysis, forming a Noyori-type catalyst with an NH functionality.[14] This included our recent report on a Milstein group developed bipy-PNN complex that can catalyze ester hydrogenation and several related transformations.[15]

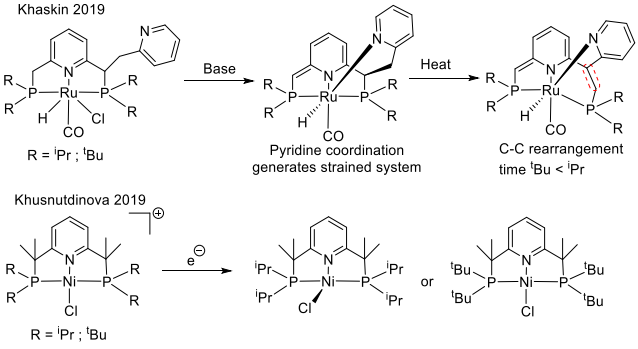

Scheme 2. Earlier reported backbone PNP pincer modified systems.

We showed that the central ring can undergo facile hydrogenation either in the presence of alcohols or hydrogen gas (Scheme 1

middle). DFT calculations suggested that catalysis proceeds via a metal-ligand assisted mechanism on a coordinatively saturated 18e$^-$ species, through a hydrogen bond network between the NH functionality and the metal bound substrate (Scheme 1 bottom). During this process, the NH bond remains intact.

When we modified the PNP ligand used in the original Milstein report by a pendant pyridine unit (Scheme 2 top), we were surprised to see a complete shutdown of catalytic activity, which was caused by a rearrangement of the backbone ligand skeleton and tighter binding of the pendant pyridine.[16]

Another modification of the PNP ligand undertaken in our group involved synthesizing bulky, tetramethyl ligands (Scheme 2 bottom) that stabilized low oxidation state nickel complexes that cannot be observed with a normal, non-methylated PNP ligand. [17] Such drastic differences in reactivity arising from slight modifications of ligand architecture suggest that it may be possible to discover a superior PNP pincer-based Ru catalyst. In this regard, the commercially available MACHO Ru PNP catalyst that does away with the pyridine in lieu of a flexible alkyl backbone is one of the best performing catalysts on the market today.[18]

After obtaining such unusual results with the original bipyPNN-Ru complex and the pyridyl modified PNP Ru complex, we decided to test the 4Me-PNP ligand on Ru and compare its reactivity to the original non-methylated system (Scheme 1 top). Based on the earlier Ni chemistry results, we expected that the 4Me-PNP ligand may form Ru(0) complexes, however, we did not expect this ligand to undergo rearrangement like the pyridyl modified PNP. If the Ru(0) complexes should be stable, they would be a relatively rare example of a pincer Ru(0) species and may provide a new and unique mechanism for alcohol dehydrogenation.

Recently, the CaRLa group found that a Ru(0) complex formed by the decomposition of the commercially available MACHO Ru catalyst was capable of interconverting to a catalytically active Ru(II) species, highlighting the possible role of Ru(0) as a resting state or intermediate in catalysis.[19]

An ^{i}PrPNP-Ru complex was in the original Milstein report in 2005,[1a] which tested only two pincer complexes for the dehydrogenative coupling of alcohols. The best performing catalyst was determined to be a diethylamine PNN complex. Chianese has recently observed that a Ru(0) imine complex formed from this commercially available Milstein catalyst as well as other imine Ru(0) complexes, are highly active pre-catalysts for ester hydrogenation. [20] The other tested complex was the symmetrical PNP Ru(II) complex, and it also behaved as a highly competent catalyst. Unfortunately, it was not further explored due to slightly inferior activity after its one trial run.

However, our group was uniquely positioned to compare reactivity of that complex to its methylated version and revisit the results. We synthesized the two previously reported pyridine-based PNP ^{i}Pr and ^{t}Bu complexes **1** and **2** using the procedure of Scheme 3, and made tetramethyl analogues **3** and **4** where MLC is blocked as the pyridine ring cannot become dearomatized (4Me-PNP).

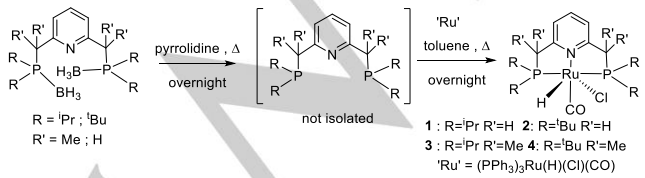

Scheme 3. Synthesis of PNP and 4Me-PNP supported complexes.

In the current paper, we show that we were able to access Ru(0) complexes with the 4Me-PNP ligands by removal of the ruthenium hydride with strong base and stabilize them for X-ray characterization by subsequent addition of CO gas. H_2 addition to deprotonated PNP-Ru(II) and 4Me-PNP-Ru(0) complexes gave trans-H_2 for the former and cis-H_2 for the latter, suggesting that MLC matters for the activation of substrates such as hydrogen gas.

We found that all complexes were active in alcohol dehydrogenation catalysis, but no clear trend could be discerned, and the most active complex was the bulkiest **4**. A detailed study of the reactivity in benzene solutions spiked with ethanol, and in neat ethanol solvent, allowed us to isolate unusual catalytic intermediates for complexes **2** and **4**, identify acetate complexes, formed via a Guerbet disproportionation of the alcohol substrate as a deactivation pathway for catalysis, and lead us to suggest that a proximal NH moiety may not be necessary for catalytic activity based on NMR reactions of **3** and **4** with ethanol in C_6D_6.

Results and Discussion

Structural Data Comparison.

In order to observe the steric influence of the four extra methyl groups on the system, we crystallized and measured data for starting complexes **1**-**4** (Figure 1; the X-ray structure of complex **2** was published previously [21]), Comparing the structures revealed that the least bulky complex **1** has ~180° P-Ru-P angles, with the bulkier species being increasingly bent. The Ru-P and Ru-H bonds are slightly elongated in both ^{t}Bu complexes compared to the ^{i}Pr ones, with the other parameters not showing significant differences or trends (i.e. the IR carbonyl stretching frequency (υ_{CO}) for complexes **1**-**4** is 1903, 1906, 1901, and 1909 cm^{-1} respectively). This suggests the electronics at the metal center are not affected by the extra four methyl groups and the reactivity of **1** and **2** can be compared to **3** and **4** in a strict MLC vs. non-MLC framework, although some distal steric effects cannot be ruled out.

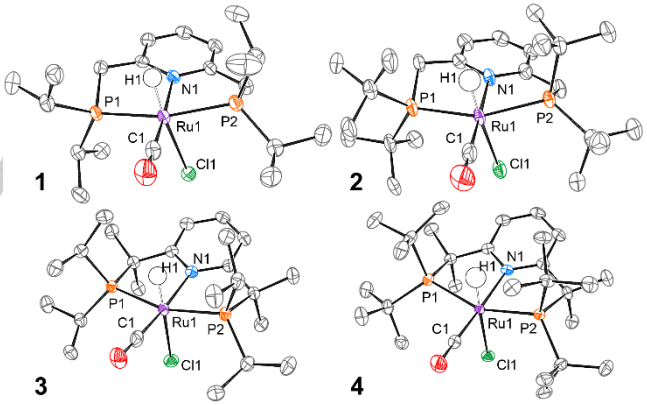

Figure 1. Structures of **1**-**4** with thermal ellipsoids at the 70 % probability level. All hydrogen atoms except the Ru1–H1 and co-crystallized CH2Cl2 molecule in the case of 1 are omitted for clarity. Selected bond distances (Å) and angles (°): Ru1–Cl1 2.5529(4), Ru1–P1 2.3113(4), Ru1–P2 2.3160(5), Ru1–N1 2.1575(15), Ru1–C1 1.838(2), Ru1–H1 1.49(2), P1–Ru1–P2 163.463(18), N1–Ru1–C1 174.83(7) for **1**; Ru1–Cl1 2.5783(7), Ru1–P1 2.3383(8), Ru1–P2 2.3355(7), Ru1–N1 2.142(2), Ru1–C1 1.841(3), Ru1–H1 1.49(4), P1–Ru1–P2 158.37(3), N1–Ru1–C1 178.45(11) for **2**; Ru1–Cl1 2.5659(4), Ru1–P1 2.2956(4), Ru1–P2 2.2993(4), Ru1–N1 2.1625(14), Ru1–C1 1.8371(19), Ru1–H1 1.48(2), P1–Ru1–P2 162.220(17), N1–Ru1–C1 172.88(7) for **3**; Ru1–Cl1 2.5938(3), Ru1–P1 2.3513(3), Ru1–P2 2.3401(3), Ru1–N1 2.1587(9), Ru1–C1 1.8366(12), Ru1–H1 1.527(19), P1–Ru1–P2 156.474(10), N1–Ru1–C1 174.34(4) for **4**.

Synthesis of Ru(0).

We next turned to the synthesis of the desired Ru(0) complexes from **3** and **4** (Scheme 4). We reasoned that a strong enough base may be able to deprotonate the complex. KO^{t}Bu did not react with the complexes at room temperature (although complete deprotonation was achieved at higher temperatures and longer time periods). Treating a solution of **3** and **4** in deuterated benzene with the stronger

potassium hexamethyl disilazide (KHMDS) gave a red solution after a few minutes, which showed the appearance of a new, symmetrical complex that did not have an associated hydride signal. The reaction was complete after half an hour and we obtained the complexes assigned as square planar Ru(0) **5** and **6** (Scheme 4) based on their diamagnetic NMR spectra, including HMQC correlations and a single ^{31}P NMR peak at 98.3 and 125.3 ppm for **5** and **6**, respectively (see SI pp.12-21). Despite filtering and solvent separation, we could not obtain complexes free of residual HMDS. Complexes **5** and **6** were extremely sensitive to small impurities in solvents or the atmosphere, unsurprisingly also decomposing rapidly in the presence of air and/or water. They could not be stored for prolonged periods of time in the solid state and proved to be unstable in solution after a few days. This was the case regardless of whether the complexes were made and stored under argon or nitrogen, suggesting that there is no stabilization effect from a possible N_2 ligand and that the complexes are tetracoordinate, and have a square planar geometry. Due to this inherent instability, elemental analysis could not be obtained, but sufficient characterization was achieved by NMR and IR spectroscopies. The 16 electron Ru(0) complexes have their aromatic protons shifted significantly upfield (Figures S16,S21).

In the ^{1}H NMR, complex **5** is well resolved, while the bulkier **6** gives broad signals that begin to resolve at -70°C in toluene-d8, suggesting hindered rotation, or the presence of a relatively long-lived agostic CH interaction between one of the Me groups and the Ru center (Figure S23).

The definite assignment of **5** and **6** as Ru(0) species was aided by their subsequent reactivity with CO and H_2, as these reaction products proved much easier to work with and characterize (Scheme 4).

Reactivity with CO gas.

Putting **5** and **6** under a CO atmosphere led to a fast color change as CO diffused into the solvent, to give dark purple and dark green solutions, which were determined to contain bis CO complexes **7** and **8**, respectively. These complexes are also unstable under reduced pressure, but proved to be indefinitely stable in solution and could be crystallized from solution as well.

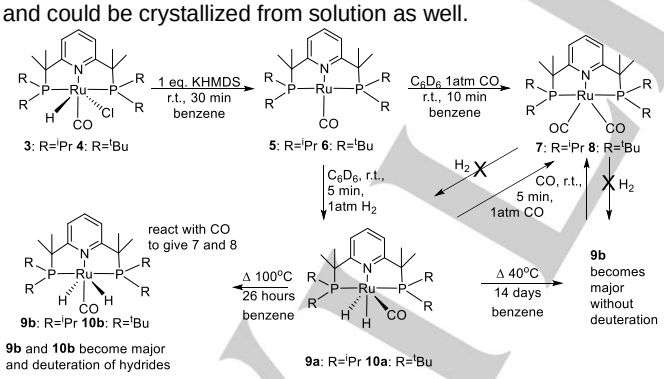

Scheme 4. Synthesis of Ru(0) complexes and their subsequent reactivity.

The bis CO complexes give two carbonyl absorptions in the IR and single peaks in the ^{31}P NMR that are shifted ca. 13 ppm downfield, 113.0 for **7** and 137.9 for **8** compared to the mono-carbonyls, as well as a symmetrical complex 1H NMR pattern (SI pp. 21-29).

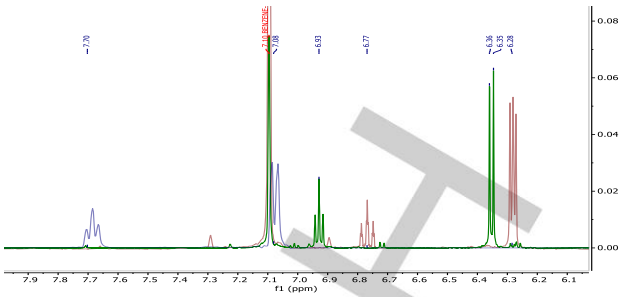

Figure 2. Aromatic NMR shifts of **3** (blue) in THF-d_8, Ru(0) mono CO **5** (green) and Ru(0) bis CO **7** (red) in C_6D_6

In the solid-state, complex **7** adopted a distorted, trigonal-bipyramidal geometry, τ5 (tau5) = 0.65, with the two phosphine arms being axial to the CO/N_{Py} plane (Figure 3). τ5 (tau5)

In contrast, the crystal structure of bulkier complex **8** showed that it was a distorted square pyramid, τ5 (tau5) = 0.10. This is an interesting parallel to the low valent Ni(I) oxidation state supported by these same bulky ligands, where the more hindered ^{t}Bu ligand led to the isolation of the square planar PNP-Ni(I)-X motif, while the less bulky ^{i}Pr version allowed for a see-saw structure.[17b]

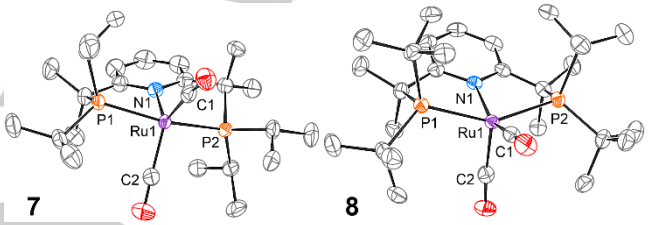

Figure 3. Structures of **7** and **8** with thermal ellipsoids at the 70 % probability level. All hydrogen atoms are omitted for clarity. Selected bond distances (Å) and angles (°): Ru1–P1 2.3047(4), Ru1–P2 2.3046(4), Ru1–N1 2.2144(13), Ru1–C1 1.8772(16), Ru1–C2 1.8734(16), O1–C1 1.1717(19), O2–C2 1.173(2), P1–Ru1–P2 160.385(15), N1–Ru1–C1 119.26(6), N1–Ru1–C2 119.57(6) for **7**; Ru1–P1 2.3360(4), Ru1–P2 2.3361(4), Ru1–N1 2.1788(13), Ru1–C1 1.8343(17), Ru1–C2 1.9177(17), O1–C1 1.177(2), O2–C2 1.159(2), P1–Ru1–P2 149.398(14), N1–Ru1–C1 155.13(6), N1–Ru1–C2 98.82(6) for **8**.

The Ru center in **8** is sitting above the basal plane by 0.4948(3) Å; however, the interaction with the axial CO is weaker, with the Ru1-C2 distance being ca. 0.08 Å longer than the distance between Ru and the equatorial carbon. This is also reflected in the longer CO bond length in the equatorial CO at 1.177(2) Å when compared to the axial CO bond length of 1.159(2) Å.

The bis-CO complexes were also stable under an atmosphere of hydrogen gas. As with the mono-carbonyl precursors, exposure to air led to rapid decolorization and decomposition.

Reactivity of 4Me-PNP complexes with Hydrogen gas.

Compounds **5** and **6** could also react with hydrogen to give cis-H_2 complexes **9a** and **10a** (Scheme 4) immediately after H_2 addition. The Ru(0) complexes are not able to heterolytically split the H_2 between the metal center and the ligand (i.e. the MLC mechanism) and can only add the H_2 ligand via homolytic splitting, thus leading to cis-H_2 complexes.

Addition of H_2 to complex **5** is accompanied by a dramatic color change from dark red to light yellow as **9a** is formed (hydride shifts at -5.91 and -13.22 ppm). Leaving a sample of **9a** at room temperature does not lead to further changes. However, heating at 100°C for 7 hours leads to significant formation of the trans-H_2 complex and almost complete deuteration of the hydride signals (integration is significantly diminished with respect to aromatic signals and trace Et_2O standard, and an HD isomer shift is observed). This appears to be the equilibrium ratio as a further 19 hours of heating

does not show any changes in the spectrum. The cis/trans ratio is difficult to determine due to the deuterium incorporation, with the RuHD and RuD_2 complexes leading to some silent ^{1}H NMR signals and broadening in the ^{31}P NMR. Heating the complex at 40°C for two weeks does however lead to the establishment of the same cis/trans equilibrium, without any deuteration of the complex hydrides, or of the dissolved H_2 signal, allowing us to establish a ratio of ~10:1.2 for the trans:cis **9b**:**9a** H_2 complex equilibrium (SI, pp. 29-43).

We found that the temperatures necessary for H/D exchange between the C_6D_6 solvent and the dissolved H_2 gas via the metal hydrides were relatively mild (> 60°C). H/D exchange between solvent and substrate via Ru(II) CH activation has been observed previously by Periana at 90-170°C.[22] Gunnoe also observed deuteration of Ru coordinated ligands by arene NMR solvents with a complex supported by a trispyrazolylborate ligand at 80°C.[23] However, we did not focus on this reactivity in the current report, as it was attendant to the exploration of acceptorless alcohol dehydrogenation catalysis.

Addition of H_2 to complex **6** leads to the formation of cis dihydride **10a** exclusively, which has very broad NMR signals. The hydrides appear as two broad peaks at -6.3 and -13.7 ppm in the ^{1}H NMR. The ^{31}P NMR peak appears in the same general location as the signal of **6** (~125 ppm), but is significantly broader with a width of ca. 6 ppm for **10a** vs. only a 2 ppm width for **6**. The reaction is accompanied by a color change to dull, light-orange. There is no further reaction at room temperature, but formation of the trans H_2 complex **10b** is seen in the ^{1}H NMR after heating at 100°C for seven hours with the trans complex also being broad and reflecting ca. 18% of all signals. However, it is impossible to determine the ratio with certainty, as there is also a degree of deuteration that takes place at this stage, and the non-hydride signals are too broad and overlapping for accurate integration. A further 19 hours of heating leads to a greater formation of **10b** at the expense of **10a** (~70% being trans assuming equal deuteration as integrated against a trace Et_2O CH_2 signal) and a clear **10b** ^{31}P NMR signal at 138.4 ppm (ca. 1 ppm broad) is also observed. Heating complex **10a** at 40°C for two weeks does not show appreciable conversion to the equilibrium mixture of **10a**/**10b** unlike with **9a**, so a non-deuterated **10b** could not be obtained in this manner.

The above experiments show that the isomerization between the cis and trans dihydride takes place, and that the complexes are capable of regenerating a Ru(0) center that can also activate sp^2 CH/D bonds of the benzene solvent. Although the dihydrides could not be purified by filtration, and under a non H_2 atmosphere were found to slowly lose H_2, leading to the highly unstable Ru(0) complexes **5** and **6**, we were able to isolate crystals of trans-H_2 **9b** from an NMR tube reaction (Figure 4), providing a solid-state example of a relatively rare Ru pincer dihydride complex.[1a, 24]

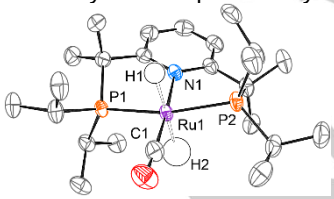

Figure 4. Structure of **9b** in the crystal with thermal ellipsoids at the 70 % probability level. All hydrogen atoms except the [Ru1–]H1 and [Ru1–]H2 and the minor disorder component are omitted for clarity. Selected bond distances (Å) and angles (°): Ru1–P1 2.2707(4), Ru1–P2 2.2968(5), Ru1–N1 2.1608(16), Ru1–C1 1.833(2), Ru1–H1 1.73(2), Ru1–H2 1.73(2), P1–Ru1–P2 162.052(19), N1–Ru1–C1 176.61(7).

Reactivity of Ru - dihydride complex with CO gas.

Replacement of the H_2 atmosphere by CO and heating at 120°C for a few minutes led to the conversion of dihydrides **9** and **10** to bis carbonyl **7** and **8** according to NMR, accompanied by the characteristic color change to dark purple and green, respectively (Scheme 4). This reaction is not reversible, as also established earlier by the reverse order addition of these gases, and **7** and **8** persisted at room temperature. Addition of the second carbonyl likely occurs via the formation of Ru(0) **5** and **6** from the dihydride complexes.

Reactivity of PNP complexes with Hydrogen gas.

The exclusive initial formation of cis-H_2 with the 4Me-PNP Ru(0) complexes, as well as the subsequent facile deuteration of the hydride signal, can be contrasted to the reactivity of non-methylated complexes **1** and **2**, where addition of base leads to previously reported dearomatized Ru(II) complexes (**11** and **12**, Scheme 5), and the subsequent formation of a trans-H_2 complex, as reported by Milstein.[1a, 24]

It has also been previously reported that addition of substrates such as alcohols,[1a, 24] acids,[6a] carbonyls,[25] and others,[26] leads to addition on the same face of the complex, to both the ligand and the metal. In the case of the addition of H_2, this same-face addition via MLC leads to re-aromatization of the ligand and formation of the trans dihydride complexes **13b** and **14b**. Based on our result with Ru(0) complexes **5** and **6**, we wanted to see if we could observe a putative Ru(0) intermediate that could form the cis dihydride complex, which would subsequently re-arrange to the trans dihydride. However, formation of a cis-H_2 complex is not likely based on the previous examples.

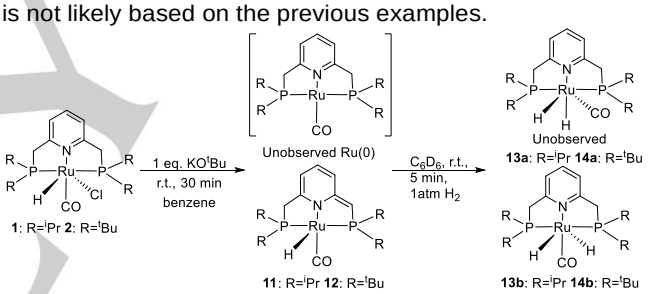

Scheme 5. Synthesis of non-methylated complexes with base and their subsequent reactivity with H_2.

We carefully repeated the H_2 addition experiments to check if a transient cis-H_2 could be detected, however, a few minutes after H_2 addition at r.t. to a C_6D_6 solution, we were unable to observe any traces of cis-H_2 complexes **13a** and **14a** by NMR, with only the trans complex seen. Thus, if the cis-H_2 complexes were formed initially, their re-arrangement to trans dihydrides would have to be much more rapid than in the case of the 4MePNP supported complexes.

13b and **14b** exhibited slight deuterium incorporation after several days of heating at 100°C into the hydride signals (ca. 40% deuteration), suggesting the elimination of H_2 and reversible activation of C_6D_6 solvent. A recent report from the Saouma group shows that **12** and **14b** exist in a temperature dependant equilibrium. [27] However, this is a much lower degree of deuteration than for the 4MePNP complexes (i.e. statistical limit after 7 hours) and after a much longer heating period. We were also unable to observe any traces of the cis complexes at this time, suggesting that there was no observable equilibrium between the trans and cis species if the latter could be accessed at all.

The above observations led us to disfavor formation of the Ru(0) isomer as a viable equilibrium species for PNP based systems, in contrast to 4Me-PNP. The cis/trans hydride ligands' isomerization, and the relatively easy formation of bis-CO complexes from the dihydrides, suggest that catalytically relevant loss of hydrogen can easily occur with the 4MePNP ligand supported complexes. Similarly, the CH

activation of the benzene solvent likely occurs via Ru(0) after reductive coupling of the H ligands.

Catalytic reactivity

We investigated the catalytic activity of complexes **1**-**4** in hexanol and butanol to establish whether the blocking of MLC has a large effect on catalytic activity. The TON was compared against a control experiment with a known, well-performing pre-catalyst H/Cl/CO PNN complex **15**,[8b] which has recently been shown to form a Noyori-type complex in-situ in the reaction mixture (see Scheme 1 for structure of activated complex).

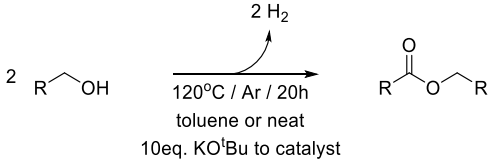

Table 1. Activity of complexes in alcohol dehydrogenative coupling catalysis reaction.

Entry	Complex	Substrate	Substrate eqiuv.	Solvent	Conversion (%)	TON
1	**15**	butanol	3000	neat	86.8	2602* +/-14
2	**15**	hexanol	3000	neat	51.1	1534* +/-580
3	**1**	hexanol	1000	toluene	11.4	114
4[a]	**1**	hexanol	1000	toluene	52.9	367* +/-146
5	**1**	hexanol	3000	neat	6.1	184* +/-14
6	**1**	butanol	3000	neat	5.7	170* +/-8
7	**2**	hexanol	3000	neat	11.4	341* +/-16
8	**2**	butanol	1000	toluene	36.0	360
9	**2**	butanol	3000	neat	12.4	371
10	**3**	hexanol	3000	neat	2.0	59* +/- 15
11	**3**	butanol	1000	toluene	11.4	114
12	**3**	butanol	3000	neat	2.6	78
13	**4**	hexanol	3000	neat	22.4	671* +/-125
14	**4**	butanol	1000	toluene	56.1	561
15	**4**	butanol	3000	neat	17.5	524

Condition- Reactions were performed in 3.0 ml of total volume of hexanol or 2.4 ml of butanol at 120°C for 16 hours with ~4-5eq. base. For reactions in toluene, 1000 eq. of alcohol was used and the volume was raised to 3 ml. Amount of catalyst was calculated according to the substrate. *TON calculated based on an average of at least two runs. a) reaction performed at 157°C.

The reaction was very clean for all five complexes (**1**-**4**, **15**), with only the starting material and the product present in the NMR after reaction completion. Perhaps somewhat expectedly, the PNN control complex **15** performed best in the reaction with almost complete conversion of butanol and half of all hexanol cleanly converted to the product after 20 hours (entries 1,2). The PNP complexes **1**-**4** all clearly performed worse at the same reaction temperature (120°C). Raising the temperature to 157°C (Entry 4) with complex **1** in toluene to replicate conditions in the original Milstein report, gave a number of byproducts. We determined the identity of the byproducts by GC/MS to be higher alcohols such as dodecanol (see SI pp. 52-59; reactions were carried out with complexes **1** and **4** in ethanol and hexanol in a closed system at 157°C), likely formed by a Guerbet reaction as reported in a recent paper by the Milstein group.[28] At 157°C, the conversion could thus be calculated based on the integration of all -CH_2 groups and an accurate TON for hexanol could also determined. Although the TON was ca. 2x higher at the higher temperature, the uncontrolled nature of the reaction is ultimately detrimental as one of the products of the Guerbet reaction is water, which can lead to production of acetate whose coordination is a deactivation pathway for catalysis in the presence of a sub-stoichiometric base.[6a] Indeed, such complexes were later isolated from model experiments (*vide infra*). The temperature was subsequently kept at 120°C to ensure controlled and repeatable catalysis. The formation of water as a side product from aldol reactions was also earlier observed in a mechanistic study on MACHO-type-Ru catalysts reported by Nguyen and Gauvin. [29] Base free catalysis with an ^{i}Pr-MACHO-Ru was explored in detail and it was ultimately found that alkoxide base can prevent the formation of acetate complexes that were determined as a deactivation pathway, or regenerate the catalyst. In this study it was also found that O_2 can lead to an acetate product as well. However, we find that our activated pyridine based pincers are sensitive to oxygen. The base free reaction for our complexes (starting with the dihydrides **9**, **10**, or dearomatized **11**, **12**) did not lead to repeatable results and often gave no TON or just a few TON in our hands, showing that excess base is required in the reaction.

Adding toluene as a co-solvent to the reaction to enable reflux did not lead to any appreciable change in TON for any of the complexes (entries 3 and 5), showing that while an open system is required for H_2 escape to drive the reaction, reflux is not necessary. Butanol and hexanol reactivity was compared to judge the effect of solvent polarity and/or substrate size on activity (entries 5,6 and 13,15). An assumption can be made that the more polar butanol solvent would stabilize charged intermediates during catalysis, or that a smaller substrate would suffer less from steric hindrance. However, we found that the choice of substrate did not play a role for all four PNP complexes while butanol did indeed give significantly better performance than hexanol in the case of the control PNN complex **15**.

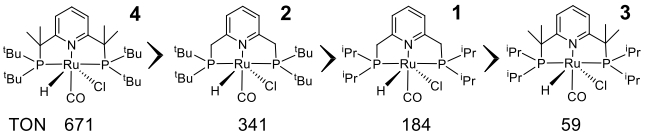

Scheme 6. Activity of synthesized complexes in catalysis.

Surprisingly, besides observing unexpected activity in the 4Me-PNP complexes that were predicted to be inactive in catalysis by MLC, we also observed divergent and unexpected TON trends for all the species. While the worst activity was observed for isopropyl 4Me-PNP complex **3** (entries 10-12), the best catalytic activity was observed for tert-butyl 4Me-PNP **4** (entries 12-15; Table 1). The ^{i}Pr complexes performed significantly worse than the ^{t}Bu complexes, with the most sterically hindered complex **4** reaching 6x as many TONs as the ^{i}PrPNP Milstein complex **1**. Which, however, in defiance of an easy trend, performed

twice better than ^{i}Pr4Me-PNP **3**. The results suggest that the reaction mechanism may differ between the complexes and is not easy to explain generally by traditional MLC. In order to gain insight into the species formed during catalysis, all four complexes were reacted with the model substrate ethanol in NMR experiments with an excess of ethanol in C_6D_6 and also in a neat ethanol solution.

Reactivity with/in ethanol

In 2012, Milstein and Montag investigated the reactivity of **2** at low temperature and found that an activated dearomatized complex in the presence of alcohol formed an alkoxy complex at -80°C, and conversion to an aldehyde and a dihydride complex was already apparent at -30°C.[24]
The aldehyde was trapped by the dearomatized complex (Scheme 7). At the time, catalytic activity with this system was not studied at the relevant conditions for catalysis, which would have to include not only experiments with excess alcohol in toluene but also reactions in neat alcohol solvent, as well as heating at catalytically relevant temperatures in order to mimic actual catalytic conditions.

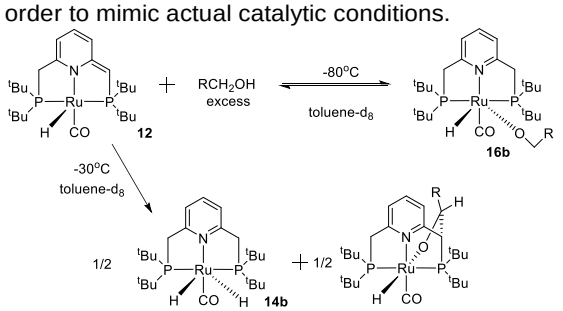

Scheme 7. Reactivity of ^{t}BuPNP complex **2** and its dearomatized activated complex **12** reported by Milstein.

To append the earlier work, the reactivity of all four complexes **1**-**4** with 5 equivalents of KOtBu (complexes **1**,**2**) or KHMDS (complexes **3**,**4**) and 40 equivalents of ethanol was observed in a closed system (NMR Young tube) in 0.4 mL of C6D6. Alternatively, 0.4 mL of ethanol were used in lieu of deuterated solvent and a solvent suppressed spectrum was obtained. The caveat is that both systems are closed and H_2 gas cannot escape, limiting the ultimate TON. However, formation of ethyl acetate (i.e. ADC catalysis) could still be observed after heating at 120°C in all but one case (complex 2); hence the system was treated as a valid proxy for observing catalytic intermediates. NMR spectra were recorded before heating and afterward. The results can be strikingly different depending on the solvent medium, highlighting the need to mimic conditions as close to those of true catalysis as possible in model experiments.

In our NMR experiments, we were able to identify the major complex after each reaction where in one case it is a Noyori-type complex with a hydrogenated backbone and in three cases it is an acetate complex that likely results from a Guerbet reaction that transforms the alcohol substrate to higher alcohols and water. [28] The acetate complexes are thermodynamic sinks that cannot reform an active catalyst without added base. [6a] Thus the TON may depend on the different rate of substrate disproportionation with each complex.

Reactivity with EtOH in C_6D_6.
The reactivity with 40 eq. of ethanol as an additive in C_6D_6 solvent is summarized in Scheme 8, and the detailed descriptions of the results for each complex can be found in the SI (pp. 60-71).

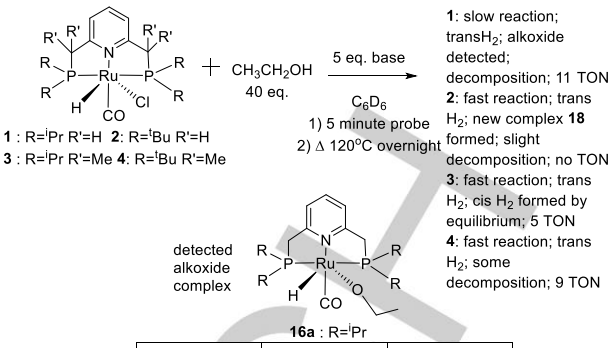

Complex	Catalysis	New Major Species
1	✓	✘
2	✘	18
3	✓	✘
4	✓	✘

Scheme 8. Summary of reactivity of complexes with 40 eq. ethanol in C_6D_6.

Catalysis in the NMR tube was observed for all complexes except **2**. While the reactions are complex, we were able to identify major species in each case. We were able to observe the alkoxide species **16a** by NMR for complex **1** only, where it was a minor species, with the major being the trans-dihydride, and disappeared over time. In the case of complex **2**, we observed the formation of a trans dihydride right away (no alkoxide detected), and its slow transformation to a new species, **18**, which was identified and isolated in later experiments. Tetra-methylated complexes **3** and **4** gave trans dihydrides after addition of ethanol substrate, that slowly isomerized and/or decomposed after prolonged heating.

Reactivity in neat EtOH.
The reactivity of **1**-**4** was also tested on a 0.01 to 0.02 mmol scale in 0.4mL. of ethanol in a Young tube. Due to solvent suppression, the spectra chiefly provided insight in the hydride region of the ^{1}H NMR and in the ^{31}P NMR. In all four reactions observed by no-D NMR, ADC catalysis (formation of ethyl acetate) was observed.
Overall Summary of reactivity in EtOH. (Scheme 9)

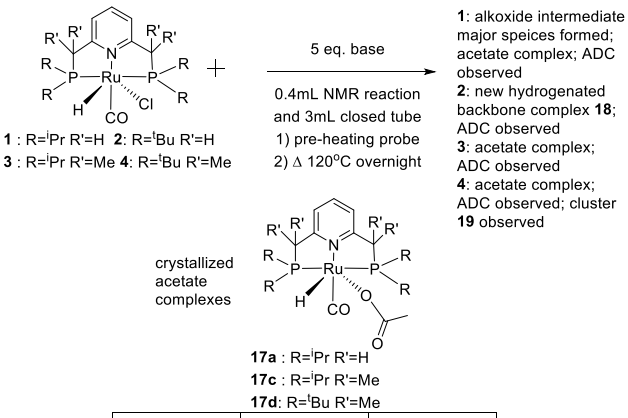

Complex	Catalysis	New Major Species
1	✓	17a
2	✓	18
3	✓	17c
4	✓	17d,19

Scheme 9. Summary of reactivity of complexes in ethanol solution.

Larger scale reactions at the 0.05 mmol scale were carried out in 3mL. of ethanol in 100mL. Schlenk flasks to isolate products. In some cases, crystallized material formed in a Schlenk flask or NMR tube was used to identify a product. After overnight heating at 120°C in the Schlenk flask, the ethanol was evaporated under high vacuum and the solids were re-dissolved in toluene, filtered through celite, the toluene was evaporated under high vacuum, and NMR obtained in C_6D_6, with the result often being a mixture, but with one major complex predominant. In all four reactions, the major complex was crystallized by slow evaporation of toluene or hexane at r.t. For detailed reaction descriptions see SI pp. 72-93

As an example of the differences with C_6D_6 solvent experiments, is the preference for the alkoxide complex **16a** in lieu of the trans-H_2 for complex **1**, which persisted in the NMR tube, while the Schlenk flask reaction showed transformation into a new acetate complex **17a** (Figure 5), with the trans dihydride that we saw in C_6D_6 not being observed. These acetate complexes were observed in all reactions except for complex **2**.

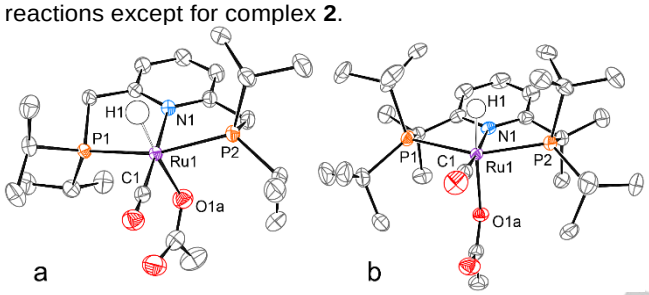

Figure 5. Structures of 1**7a** (a) and **17d** (b) in the crystals with thermal ellipsoids at the 70 % probability level. All hydrogen atoms except the [Ru1–]H1 are omitted for clarity. Selected bond distances (Å) and angles (°): Ru1–P1 2.3141(3), Ru1–P2 2.3159(3), Ru1–O1a 2.1998(11), Ru1–N1 2.1560(12), Ru1–C1 1.8368(14), Ru1–H1 1.54(2), P1–Ru1–P2 161.084(13), N1–Ru1–C1 176.86(5) for 1**7a**; Ru1–P1 2.3460(3), Ru1–P2 2.3440(3), Ru1–O1a 2.2160(9), Ru1–N1 2.1704(11), Ru1–C1 1.8332(13), Ru1–H1 1.499(17), P1–Ru1–P2 157.521(12), N1–Ru1–C1 173.55(5) for 1**7d**. See SI for structure of **17c**.

Complex **2** transformed clearly into the new species **18** both in the NMR and in the Schlenk flask where it could be easily isolated and characterized. In **18**, the backbone of the pyridine ring is hydrogenated (Figure 6). However, the arms of the ligand are deprotonated. This type of hydrogenated ligand complex was only obtained from **2** and not the other three complexes.

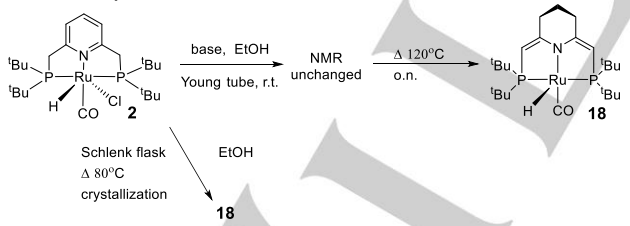

Scheme 10. Reactivity of complex **2** in neat ethanol.

Counterintuitively, complex **18** prefers to be a 16-electron species despite the large concentration of ethanol. This complex was also observed in the in C_6D_6 reaction, where it can be detected as a minor complex after overnight heating. That reaction was the only one out of the four that did not show catalytic formation of EtOAc and the only one to have such an extremely upfield shifted hydride peak that only later could be identified as **18**. It's not clear why **2** reacts so differently compared to the other three complexes, but it highlights that small changes in sterics and electronics can cause dramatic changes in catalytic pathways and would also mean that results with one system should not be generalized to all.

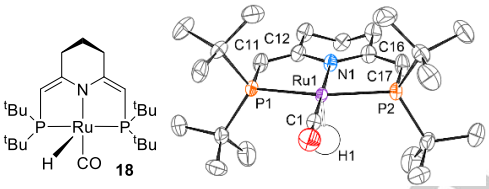

Figure 6. Structure of **18** in the crystal with thermal ellipsoids at the 70 % probability level. All hydrogen atoms except the [Ru1–]H1 and the minor disorder component are omitted for clarity. Selected bond distances (Å) and angles (°): Ru1–P1 2.3380(3), Ru1–P2 2.3298(3), Ru1–N1 2.1155(11), Ru1–C1 1.8377(13), Ru1–H1 1.51(2), C11–C12 1.3570(19), C16–C17 1.363(2), P1–Ru1–P2 163.827(13), N1–Ru1–C1 175.12(5).

For complex **3**, the reaction was slow and required heating. After one hour, we were able to observe the cis dihydride **9a** in the ethanol no-D NMR, with the acetate complex **17c** forming after prolonged heating. The larger scale Schlenk flask experiment allowed us to isolate **17c**.

In contrast to **3**, complex **4** reacted much more rapidly and gave trans dihydride **10b** already at room temperature after mixing. After heating we were able to detect two complexes by NMR, which were characterized as **17d** and **19**. The larger scale experiment led to the isolation of these two species with full characterization for **17d** (Figure 5) and an X-ray structure for **19** (Figure 7). The latter compound is a very interesting and unprecedented cluster that crystallized in the ethanol solution and was isolated from the walls of the Schlenk flask.

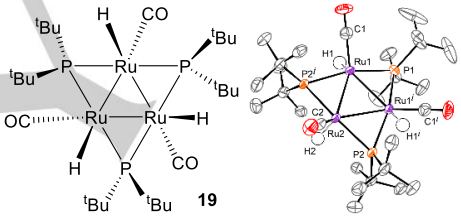

Figure 7. Structure of **19** in the crystal with thermal ellipsoids at the 70 % probability level. All hydrogen atoms except the [Ru1–]H1 and [Ru2–]H2 and the minor disorder component are omitted for clarity. The atoms marked by superscripts *i* are related by the mirror plane (–*x*+1, *y*, *z*). Selected bond distances (Å) and angles (°): Ru1–Ru1^i 2.6656(6), Ru1–Ru2 2.6548(5), Ru1–P1 2.3343(15), Ru1–P2^i 2.3409(12), Ru2–P2 2.3437(11), Ru2–P2^i 2.3437(11), Ru1–C1 1.841(5), Ru2–C2 1.823(8), Ru1–H1 1.40(6), Ru2–H2 1.40(6), Ru2–Ru1–Ru1^i 59.866(9), Ru1–Ru2–Ru1^i 60.269(18), Ru1–P1–Ru1^i 69.63(5), Ru2–P2–Ru1^i 69.04(3).

This cluster bears some resemblance to the carbonyl/phosphine clusters with bridging hydrides that were explored, including for their catalytic properties, by the groups of Boettcher,[30] Sappa,[31] and others,[32] with the difference being the much lower saturation of Ru centers by phosphine and CO ligands in **19**. It may be of interest for further catalytic exploration due to its high hydride and relatively low CO content. The obvious problem is that it is not clear how to obtain the cluster without it being a decomposition product of **4** in ethanol and we did not obtain enough material to attempt catalysis or to obtain a clean NMR (although a hydride shift at -6.3 ppm (broad triplet) in C_6D_6 could be assigned, Figure S113) before decomposition under air. It's likely that the cluster decomposes under high vacuum, leading to the large number of hydride and phosphine shifts observed in the residue after the Schlenk flask reaction.

The cluster could be one of the major decomposition pathways for **4** in ethanol and highlights that the mechanism of catalysis and stability of even the basic architecture of PNP complexes cannot be taken for granted under the reductive catalytic conditions. The decomposition may be aided by the severe steric strain of **4** compared to the other three complexes.

Complex **4** was the best performing catalyst (Table 1) and it may be tempting to assign the credit to **19**, which does not have analogues with the other three complexes. However, due to the isolation of acetate complex **17d**, the relatively clean NMR tube reactions, and the precedent with complexes **1** and **3**, we currently assign a greater probability to a more traditional, non-cluster catalyzed process for alcohol dehydrogenation with **4**.

Summary of reactivity and catalysis.

It was surprising to us that all four methylated and non-methylated complexes were active in ADC catalysis, seemingly abrogating the traditional requirement for the MLC mechanistic pathway. In fact, the most hindered complex **4** with four methyl groups on the arms, was the most active catalyst out of the four, while the worst performing one was its iPr substituted cousin **3**. The prolific range of catalytic reactivity is in striking contrast to our earlier result (Scheme 2), which found that addition of just one pyridine methyl moiety on the arm of a PNP complex completely shuts down catalysis by allowing for ligand rearrangement and the formation of a relatively weak Ru-N bond.

Another unexpected result was the different manner in which complex **2** reacts with ethanol in contrast to the other complexes. We were not able to find even a hint of a similar hydrogenated backbone species such as **18**, with its characteristic upfield hydride shift and lack of associated aromatic signals, for the other three complexes. Reactions of complexes **1**, **3**, and **4** led to crystallization of acetate complexes as the major species in Schlenk flask post-reaction mixtures, while the reaction of **2** did not show even a trace of the acetate complex based on a careful examination of the hydride region.

Lastly, complex **4** also decomposed to give upfield shifted ^{31}P NMR peaks that were not observed in the other three reactions, and crystals isolated from an ethanol solution revealed the presence of a novel and unusual cluster species **19**, while the acetate complex was isolated from the toluene soluble residue.

It would be tempting to assign greater reactivity to one pathway, such as formation of **19** or **18** as the superior catalyst, while the pathway via traditional MLC is disfavored. However, **18** or **19** were obtained in small amounts and a preliminary test with **18** showed lower catalytic activity than the parent complex **2**. The control reaction with PNN complex **15**, earlier shown by us to proceed via a ligand hydrogenation mechanism and NH bond assistance during catalysis also shows much greater activity than any of the herein tested PNP complexes. Despite this, the current results from reactions of ethanol in C_6D_6 where limited or no decomposition took place (complexes **3** and **4**) with TON observed, show that an NH moiety may not be strictly necessary for catalysis.

The results from the current study and our earlier two papers, as well as those by others,[20, 33] show that ADC is a versatile reaction that may proceed by several different pathways depending on the complex, or can be completely shut down by a rather trivial ligand modification. In this regard, the presence of acetate complexes formed in super dry ethanol (Supelco, max 1 ppm H_2O), where the maximum water amount present would have been several times less than the amount of excess base, shows that a Guerbet reaction is an important consideration for catalyst deactivation. As shown previously, excess base allows for trapping of formed acetates and regeneration of the active species.[6a] Designing complexes capable of easily decoordinating acetate, or that are completely inactive in disproportionation, or accepting the necessity of a large excess of base with known catalytic systems that may have performed poorly if activated with only 1-2 eq. of base, may lead to greater TONs.

In this regard, it's interesting to compare Entries 3 and 4 of Table 1 of catalysis with complex **1** at 120°C and 157°C respectively. The former transformation was a clean conversion of hexanol hexyl hexanoate. The latter higher temperature gave a 3x higher TON, but there were a number of higher chain alcohols and esters (that could be confirmed by GC/MS) that were identified as byproducts of the Guerbet reaction. There is likely a trade-off with a lower temperature being beneficial in not forming as much acetate, but the acetate coordinating more strongly. At higher temperatures, the disproportionation to higher alcohol and water is more prominent, as we form enough of them to detect them by GC/MS (See SI pp. 52-59), but it may also be easier to decoordinate acetates as long as their concentration is low enough and there is enough base.

Conclusion

We synthesized methylated PNP complexes **3** and **4** to test the validity of the metal-ligand cooperative (MLC) catalysis pathway in alcohol dehydrogenation catalysis and compared activity with previously reported non-methylated **1** and **2**. At first, we explored the reactivity of the new complexes and found that we could form 16 and 18 electron Ru(0) species. These are relatively rare, well-defined examples of pincer Ru(0) complexes. We were also able to perform oxidative addition reactions to the 16 electron square planar Ru(0) which gave cis-H_2 complexes as expected from a non-MLC process, while the non-methylated complexes gave trans-H_2 products exclusively.

In comparing ADC catalysis, we found that all four complexes performed differently, and no specific trend could be discerned. In ethanol model reactions, complex **2** was, in contrast to the other three species, uniquely transformed to a hydrogenated backbone complex **18**, which is the first example of a 16 electron Ru(II) complex that is stable in ethanol solution. The other three complexes gave acetate species as the major products, hinting at a common deactivation pathway by alcohol disproportionation (Guerbet process). However, all reactions also gave a number of species that cannot be conclusively identified, highlighted by the isolation of the unusual Ru cluster **19** from solutions of **4**. Based on the above, we can infer that MLC is not strictly required for ADC and the exact mechanism depends on the complex, with dramatic differences being observed even by slightly changing substituents on the phosphine.

In the future, we would like to synthesize cluster **19** by a different method and test its properties. We are also currently exploring basic organometallic reactions of Ru(0) complexes **5** and **6**. Finally, we also found that blocking of MLC does not mean diminished activity in catalysis. It also allows for more efficient CD activation of benzene solvent and we would like to utilize these bulky ligands for metals which have been shown to be more effective for CH activation reactions and explore further CH functionalization applications.

Conflicts of interest

There are no conflicts to declare.

Acknowledgements

The authors acknowledge Professor Dmitry Gusev and Professor Julia Khusnutdinova for valuable discussions and suggestions on the manuscript, and Dr. Michael C. Roy for help with mass spectral measurement. R. R. F. performed

crystal structure determination within the statements for Kazan Scientific Center of RAS.

Keywords: Ruthenium, Catalysis, Metal-Ligand Cooperation.

[1] a) J. Zhang, G. Leitus, Y. Ben-David, D. Milstein, *Journal of the American Chemical Society* **2005**, *127*, 10840-10841; b) J. Zhang, G. Leitus, Y. Ben-David, D. Milstein, *Angewandte Chemie* **2006**, *118*, 1131-1133; c) C. Gunanathan, D. Milstein, *Science (Washington, DC, U. S.)* **2013**, *341*, 249; d) J. R. Khusnutdinova, D. Milstein, *Angew. Chem., Int. Ed.* **2015**, *54*, 12236-12273; e) L. Saudan, P. Dupau, J.-J. Riedhauser, P. Wyss, Firmenich S. A., Switz. . **2006**, p. 40pp; f) L. A. Saudan, C. Saudan, C. Becieux, P. Wyss, *Angew. Chem., Int. Ed.* **2007**, *46*, 7473-7476.

[2] C. Gunanathan, Y. Ben-David, D. Milstein, *Science (Washington, DC, U. S.)* **2007**, *317*, 790-792.

[3] a) E. Balaraman, B. Gnanaprakasam, L. J. W. Shimon, D. Milstein, *J. Am. Chem. Soc.* **2010**, *132*, 16756-16758; b) J. R. Cabrero-Antonino, E. Alberico, H.-J. Drexler, W. Baumann, K. Junge, H. Junge, M. Beller, *ACS Catal.* **2016**, *6*, 47-54; c) J. M. John, S. H. Bergens, *Angew. Chem., Int. Ed.* **2011**, *50*, 10377-10380, S10377/10371-S10377/10324; d) S. Kar, M. Rauch, A. Kumar, G. Leitus, Y. Ben-David, D. Milstein, *ACS Catal.* **2020**, *10*, 5511-5515; e) L. Shi, X. Tan, J. Long, X. Xiong, S. Yang, P. Xue, H. Lv, X. Zhang, *Chem. - Eur. J.* **2017**, *23*, 546-548.

[4] a) B. Gnanaprakasam, J. Zhang, D. Milstein, *Angew. Chem., Int. Ed.* **2010**, *49*, 1468-1471, S1468/1461-S1468/1467; b) N. J. Oldenhuis, V. M. Dong, Z. Guan, *Tetrahedron* **2014**, *70*, 4213-4218.

[5] a) V. Cherepakhin, T. J. Williams, *ACS Catal.* **2020**, *10*, 56-65; b) F.-L. Yang, Y.-H. Wang, Y.-F. Ni, X. Gao, B. Song, X. Zhu, X.-Q. Hao, *Eur. J. Org. Chem.* **2017**, *2017*, 3481-3486; c) S. Agrawal, M. Lenormand, B. Martin-Matute, *Org. Lett.* **2012**, *14*, 1456-1459; d) E. Balaraman, D. Srimani, Y. Diskin-Posner, D. Milstein, *Catal. Lett.* **2015**, *145*, 139-144.

[6] a) E. Balaraman, E. Khaskin, G. Leitus, D. Milstein, *Nat. Chem.* **2013**, *5*, 122-125; b) D. Gong, B. Hu, D. Chen, *Dalton Trans.* **2019**, *48*, 8826-8834; c) H.-M. Liu, L. Jian, C. Li, C.-C. Zhang, H.-Y. Fu, X.-L. Zheng, H. Chen, R.-X. Li, *J. Org. Chem.* **2019**, *84*, 9151-9160; d) P. Garrido-Barros, I. Funes-Ardoiz, P. Farras, C. Gimbert-Surinach, F. Maseras, A. Llobet, Georg Thieme Verlag, **2018**, pp. 63-80; e) J.-H. Choi, L. E. Heim, M. Ahrens, M. H. G. Prechtl, *Dalton Trans.* **2014**, *43*, 17248-17254; f) E. W. Dahl, T. Louis-Goff, N. K. Szymczak, *Chem. Commun. (Cambridge, U. K.)* **2017**, *53*, 2287-2289; g) L. Zhang, D. H. Nguyen, G. Raffa, X. Trivelli, F. Capet, S. Desset, S. Paul, F. Dumeignil, R. M. Gauvin, *ChemSusChem* **2016**, *9*, 1413-1423.

[7] a) S. Ramakrishnan, K. M. Waldie, I. Warnke, A. G. De Crisci, V. S. Batista, R. M. Waymouth, C. E. D. Chidsey, *Inorg. Chem.* **2016**, *55*, 1623-1632; b) S. Wesselbaum, T. vom Stein, J. Klankermayer, W. Leitner, *Angew. Chem., Int. Ed.* **2012**, *51*, 7499-7502, S7499/7491-S7499/7499.

[8] a) B. Chatterjee, C. Gunanathan, *Org. Lett.* **2015**, *17*, 4794-4797; b) E. Khaskin, D. Milstein, *ACS Catal.* **2013**, *3*, 448-452.

[9] A. Kaithal, M. Schmitz, M. Hoelscher, W. Leitner, *ChemCatChem* **2019**, *11*, 5287-5291.

[10] a) E. Khaskin, D. Milstein, *Chem. Commun. (Cambridge, U. K.)* **2015**, *51*, 9002-9005; b) M. B. Chaudhari, G. S. Bisht, P. Kumari, B. Gnanaprakasam, *Org. Biomol. Chem.* **2016**, *14*, 9215-9220; c) T. Vojkovsky, S. Deolka, S. Stepanova, M. C. Roy, E. Khaskin, *ACS Catal.* **2020**, *10*, 6810-6815.

[11] T. C. Jankins, R. R. Fayzullin, E. Khaskin, *Organometallics* **2018**, *37*, 2609-2617.

[12] a) S. A. Morris, D. G. Gusev, *Angew. Chem., Int. Ed.* **2017**, *56*, 6228-6231; b) D. Spasyuk, D. G. Gusev, *Organometallics* **2012**, *31*, 5239-5242; c) D. Spasyuk, S. Smith, D. G. Gusev, *Angew. Chem., Int. Ed.* **2013**, *52*, 2538-2542; d) G. A. Filonenko, M. J. B. Aguila, E. N. Schulpen, R. van Putten, J. Wiecko, C. Mueller, L. Lefort, E. J. M. Hensen, E. A. Pidko, *J. Am. Chem. Soc.* **2015**, *137*, 7620-7623; e) E. Fogler, J. A. Garg, P. Hu, G. Leitus, L. J. W. Shimon, D. Milstein, *Chem. - Eur. J.* **2014**, *20*, 15727-15731.

[13] T. P. Goncalves, I. Dutta, K.-W. Huang, *Chem. Commun. (Cambridge, U. K.)* **2021**, *57*, 3070-3082.

[14] a) R. Langer, I. Fuchs, M. Vogt, E. Balaraman, Y. Diskin-Posner, L. J. W. Shimon, Y. Ben-David, D. Milstein, *Chem. - Eur. J.* **2013**, *19*, 3407-3414; b) T. Miura, I. E. Held, S. Oishi, M. Naruto, S. Saito, *Tetrahedron Lett.* **2013**, *54*, 2674-2678; c) T. Miura, M. Naruto, K. Toda, T. Shimomura, S. Saito, *Sci Rep* **2017**, *7*, 1586; d) P. A. Dub, J. C. Gordon, *Nature Reviews Chemistry* **2018**, *2*, 396-408.

[15] L. N. Dawe, M. Karimzadeh-Younjali, Z. Dai, E. Khaskin, D. G. Gusev, *J. Am. Chem. Soc.* **2020**, *142*, 19510-19522.

[16] S. Deolka, N. Tarannam, R. R. Fayzullin, S. Kozuch, E. Khaskin, *Chem. Commun. (Cambridge, U. K.)* **2019**, *55*, 11350-11353.

[17] a) S. Lapointe, E. Khaskin, R. R. Fayzullin, J. R. Khusnutdinova, *Organometallics* **2019**, *38*, 4433-4447; b) S. Lapointe, E. Khaskin, R. R. Fayzullin, J. R. Khusnutdinova, *Organometallics* **2019**, *38*, 1581-1594.

[18] W. Kuriyama, T. Matsumoto, O. Ogata, Y. Ino, K. Aoki, S. Tanaka, K. Ishida, T. Kobayashi, N. Sayo, T. Saito, *Organic Process Research & Development* **2012**, *16*, 166-171.

[19] a) A. Anaby, M. Schelwies, J. Schwaben, F. Rominger, A. S. K. Hashmi, T. Schaub, *Organometallics* **2018**, *37*, 2193-2201; b) D. J. Tindall, M. Menche, M. Schelwies, R. A. Paciello, A. Schaefer, P. Comba, F. Rominger, A. S. K. Hashmi, T. Schaub, *Inorg. Chem.* **2020**, *59*, 5099-5115.

[20] T. He, J. C. Buttner, E. F. Reynolds, J. Pham, J. C. Malek, J. M. Keith, A. R. Chianese, *J. Am. Chem. Soc.* **2019**, *141*, 17404-17413.

[21] A. Eizawa, S. Nishimura, K. Arashiba, K. Nakajima, Y. Nishibayashi, *Organometallics* **2018**, *37*, 3086-3092.

[22] a) K. J. H. Young, K. S. Lokare, C. H. Leung, M.-J. Cheng, R. J. Nielsen, N. A. Petasis, W. A. Goddard, III, R. A. Periana, *J. Mol. Catal. A: Chem.* **2011**, *339*, 17-23; b) B. G. Hashiguchi, K. J. H. Young, M.

Yousufuddin, W. A. Goddard, R. A. Periana, *Journal of the American Chemical Society* **2010**, *132*, 12542-12545.

[23] Y. Feng, M. Lail, N. A. Foley, T. B. Gunnoe, K. A. Barakat, T. R. Cundari, J. L. Petersen, *J. Am. Chem. Soc.* **2006**, *128*, 7982-7994.

[24] M. Montag, J. Zhang, D. Milstein, *J. Am. Chem. Soc.* **2012**, *134*, 10325-10328.

[25] a) C. A. Huff, J. W. Kampf, M. S. Sanford, *Chemical Communications* **2013**, *49*, 7147; b) M. Vogt, A. Nerush, Y. Diskin-Posner, Y. Ben-David, D. Milstein, *Chem. Sci.* **2014**, *5*, 2043-2051; c) G. A. Filonenko, D. Smykowski, B. M. Szyja, G. Li, J. Szczygieł, E. J. M. Hensen, E. A. Pidko, *ACS Catalysis* **2015**, *5*, 1145-1154.

[26] a) E. Khaskin, M. A. Iron, L. J. W. Shimon, J. Zhang, D. Milstein, *J. Am. Chem. Soc.* **2010**, *132*, 8542-8543; b) J. Bootsma, B. Guo, J. G. De Vries, E. Otten, *Organometallics* **2020**, *39*, 544-555; c) B. Guo, J. G. De Vries, E. Otten, *Chemical Science* **2019**, *10*, 10647-10652; d) L. E. Eijsink, S. C. P. Perdriau, J. G. de Vries, E. Otten, *Dalton Trans.* **2016**, *45*, 16033-16039; e) A. Nerush, M. Vogt, U. Gellrich, G. Leitus, Y. Ben-David, D. Milstein, *J. Am. Chem. Soc.* **2016**, *138*, 6985-6997; f) S. Perdriau, D. S. Zijlstra, H. J. Heeres, J. G. de Vries, E. Otten, *Angew. Chem., Int. Ed.* **2015**, *54*, 4236-4240; g) Y. Sun, C. Koehler, R. Tan, V. T. Annibale, D. Song, *Chemical Communications* **2011**, *47*, 8349; h) M. Vogt, A. Nerush, M. A. Iron, G. Leitus, Y. Diskin-Posner, L. J. W. Shimon, Y. Ben-David, D. Milstein, *Journal of the American Chemical Society* **2013**, *135*, 17004-17018; i) G. A. Filonenko, E. Cosimi, L. Lefort, M. P. Conley, C. Copéret, M. Lutz, E. J. M. Hensen, E. A. Pidko, *ACS Catalysis* **2014**, *4*, 2667-2671.

[27] C. L. Mathis, J. Geary, Y. Ardon, M. S. Reese, M. A. Philliber, R. T. VanderLinden, C. T. Saouma, *J. Am. Chem. Soc.* **2019**, *141*, 14317-14328.

[28] Y. Xie, Y. Ben-David, L. J. W. Shimon, D. Milstein, *Journal of the American Chemical Society* **2016**, *138*, 9077-9080.

[29] D. H. Nguyen, X. Trivelli, F. Capet, Y. Swesi, A. Favre-Reguillon, L. Vanoye, F. Dumeignil, R. M. Gauvin, *ACS Catal.* **2018**, *8*, 4719-4734.

[30] a) H.-C. Bottcher, M. Graf, C. Wagner, *Phosphorus, Sulfur Silicon Relat. Elem.* **2001**, *168-169*, 509-512; b) H.-C. Bottcher, M. Graf, K. Merzweiler, C. Bruhn, *Polyhedron* **1998**, *17*, 3433-3438; c) M. Graf, K. Merzweiler, C. Bruhn, H.-C. Bottcher, *J. Organomet. Chem.* **1998**, *553*, 371-378.

[31] a) M. Castiglioni, R. Giordano, E. Sappa, *J. Organomet. Chem.* **1988**, *342*, 97-109; b) M. Castiglioni, R. Giordano, E. Sappa, *J. Organomet. Chem.* **1988**, *342*, 111-127; c) M. Castiglioni, R. Giordano, E. Sappa, *J. Organomet. Chem.* **1989**, *362*, 399-410; d) M. Castiglioni, R. Giordano, E. Sappa, *J. Organomet. Chem.* **1989**, *369*, 419-431.

[32] a) G. Suss-Fink, I. Godefroy, M. Faure, A. Neels, H. Stoeckli-Evans, *J. Cluster Sci.* **2001**, *12*, 35-48; b) J. A. Cabeza, F. J. Lahoz, A. Martin, *Organometallics* **1992**, *11*, 2754-2756; c) J. S. Field, R. J. Haines, F. Mulla, *J. Organomet. Chem.* **1990**, *389*, 227-249; d) L. M. Bullock, J. S. Field, R. J. Haines, E. Minshall, M. H. Moore, F. Mulla, D. N. Smit, L. M. Steer, *J. Organomet. Chem.* **1990**, *381*, 429-456; e) N. Lugan, G. Lavigne, J. J. Bonnet, R. Reau, D. Neibecker, I. Tkatchenko, *J. Am. Chem. Soc.* **1988**, *110*, 5369-5376; f) R. P. Rosen, G. L. Geoffroy, C. Bueno, M. R. Churchill, R. B. Ortega, *J. Organomet. Chem.* **1983**, *254*, 89-103.

[33] J. Pham, C. E. Jarczyk, E. F. Reynolds, S. E. Kelly, T. Kim, T. He, J. M. Keith, A. R. Chianese, *ChemRxiv* **2021**, 1-35.

Entry for the Table of Contents

Insert graphic for Table of Contents here.

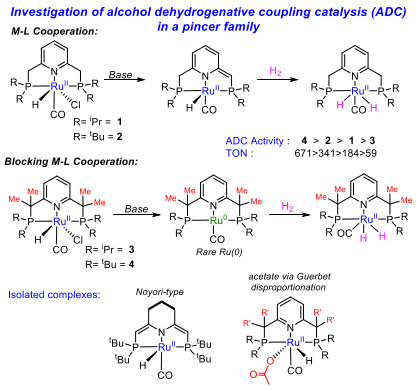

We synthesized two 4Me-PNP Ru complexes and compared their catalytic performance against two traditional analogues used in acceptorless alcohol dehydrogenation catalysis, leading us to identify a common deactivation pathway. The 4Me-PNP complexes, which do not undergo dearomatization upon addition of base, also allowed us to obtain rare, albeit unstable, 16 electron mono CO Ru(0), and their subsequent Ru(II) reaction products.

Institute and/or researcher Twitter usernames: @EugeneKhaskin